

# Properties and perspectives of digital holographic technology in bio-detection.



This project has received funding from the European Union's Horizon 2020 research and innovation programme, under grant agreement No 101021723.

János Pálhalmi<sup>1</sup> (CA), Béla Mihalik<sup>2</sup>, Francesca Pennati<sup>3</sup>, Alessandro Molani<sup>3</sup>, Andrea Aliverti<sup>3</sup>, Abhinav Sharma<sup>4</sup>, Paul Claassen<sup>4</sup>, Thijs Withaar<sup>4</sup>, Anna Mezői<sup>1</sup>, Mariana L. Ferrari<sup>5</sup>, Rémy Artus<sup>5</sup>, Györgyi Bela<sup>2</sup>, Michel Zayet<sup>6</sup>, Marcin Niemcewicz<sup>7</sup> (co-CA)

<sup>1</sup>DataSenseLabs Ltd., Budapest, Hungary; <sup>2</sup>Ideas Science Ltd., Budapest, Hungary; <sup>3</sup>Dipartimento di Elettronica, Informazione e Bioingegneria, Politecnico di Milano, Milan, Italy; <sup>4</sup>Sioux Technologies B.V, Eindhoven, Netherlands; <sup>5</sup>Institut Pasteur, Biological Resource Center - ICAREB, Paris, France; <sup>6</sup>DMI - Communication, End Users & Training, Lyon, France; <sup>7</sup>Biohazard Prevention Centre, Faculty of Biology and Environmental Protection, University of Lodz, Lodz Poland

## Introduction

Concerns of biological terror events and the appearance of new pathogens have generated an intensive demand for rapid, on-site applicable bio-detection methods which can be integrated into either the preventive or the intervention related decision-making process of CBRNE first responders. The combination of optical and digital holographic (DH) detection methods offers the possibility of overcoming the problem of rapid response time and connectivity with other existing sub-systems.

In the present study, results of single frame simulations carried out under ideal conditions were used to define the theoretical limit of detection in the case of in-line, point source digital holography. Fundamental statistical methods were used to describe the properties of the raw holographic signatures of two example bacterial strains to uncover the potential of the system as a direct measurement method.

## Conclusion

Detectability of simulated particles and bacterial objects in the  $\mu\text{m}$  range is within 95% coverage probability under ideal conditions. This establishes the possibility of detecting changes with high confidence in the distribution of airborne particle diameter within the dimension of bacteria.

Analysis of the periodicity within the intensity profiles of simulated particles indicates that the reliable limit of detection is within the submicron range (above 125 nm) which provides the possibility of nanoparticle detection as well, by applying the appropriate signal processing, digital and optical filtering methods.

Based on the current results, the DH measurement methodology is capable of quick detection of changes in the distribution of airborne nano- and micro-particles, which enables the integration of DH technology by the first-responders on-site, for quick decision making.

### Holographic Representation of Individual Particles

**Fig.1.** Simulated Holographic Representation particle diameter = 2 micrometer

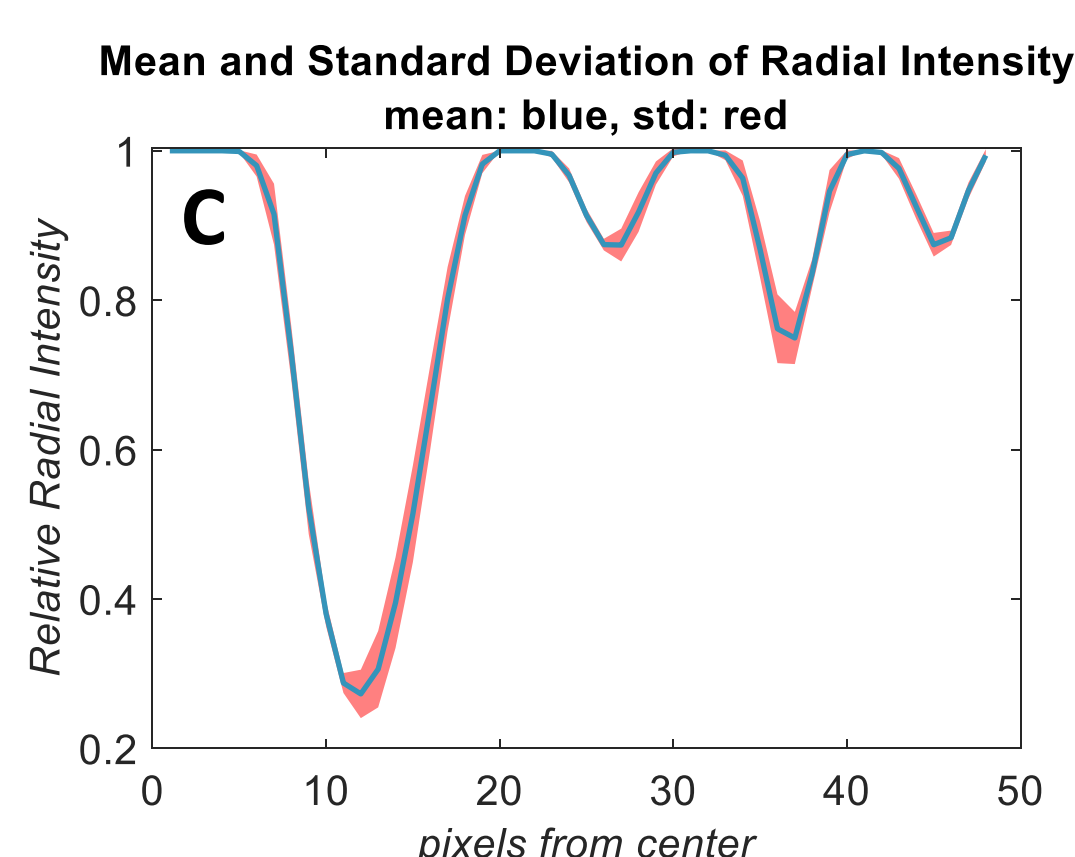
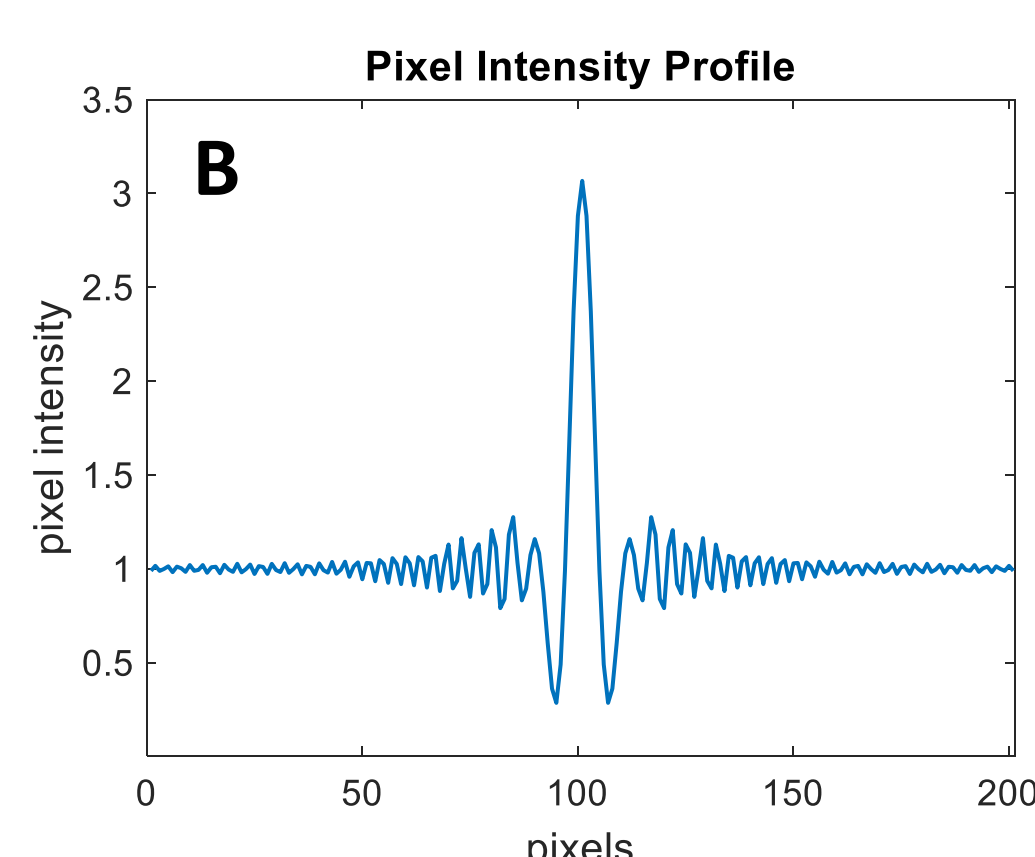
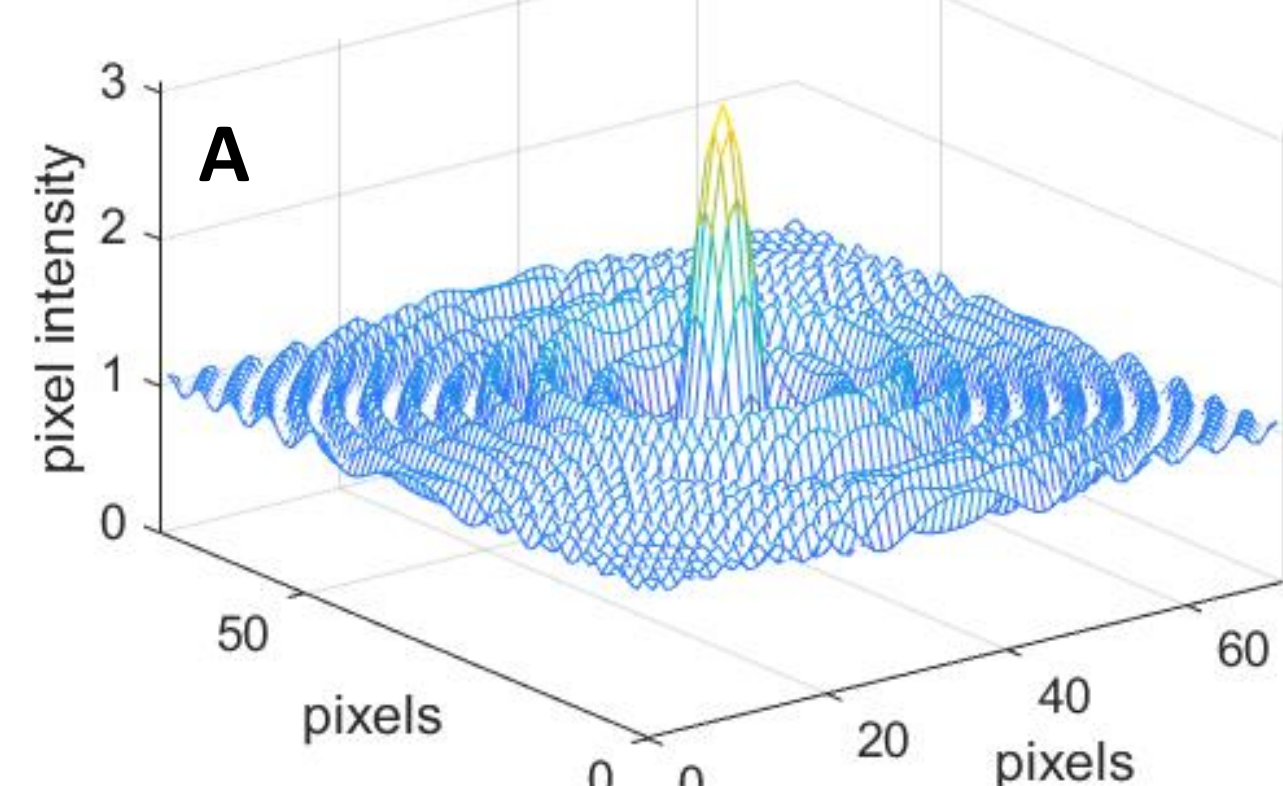


**Fig. 1. and 2. A, B, C.**

Representation of the holographic raw data output of in-line, point source Simulation according to the 'Mie' model.

**Fig.1.A.:** 3D plot of a particle with 2  $\mu\text{m}$  diameter. **Fig.1.B.:** Pixel intensity profile of the same particle with 2  $\mu\text{m}$  diameter. **Fig.1.C.:** Mean and standard deviation of the polar coordinate representation of same particle with 2  $\mu\text{m}$  diameter.

### Statistical signature of digital holographic images

**Fig.3.** Digital holographic signature of *Candida Albicans* (A) and *Escherichia Coli* (B).

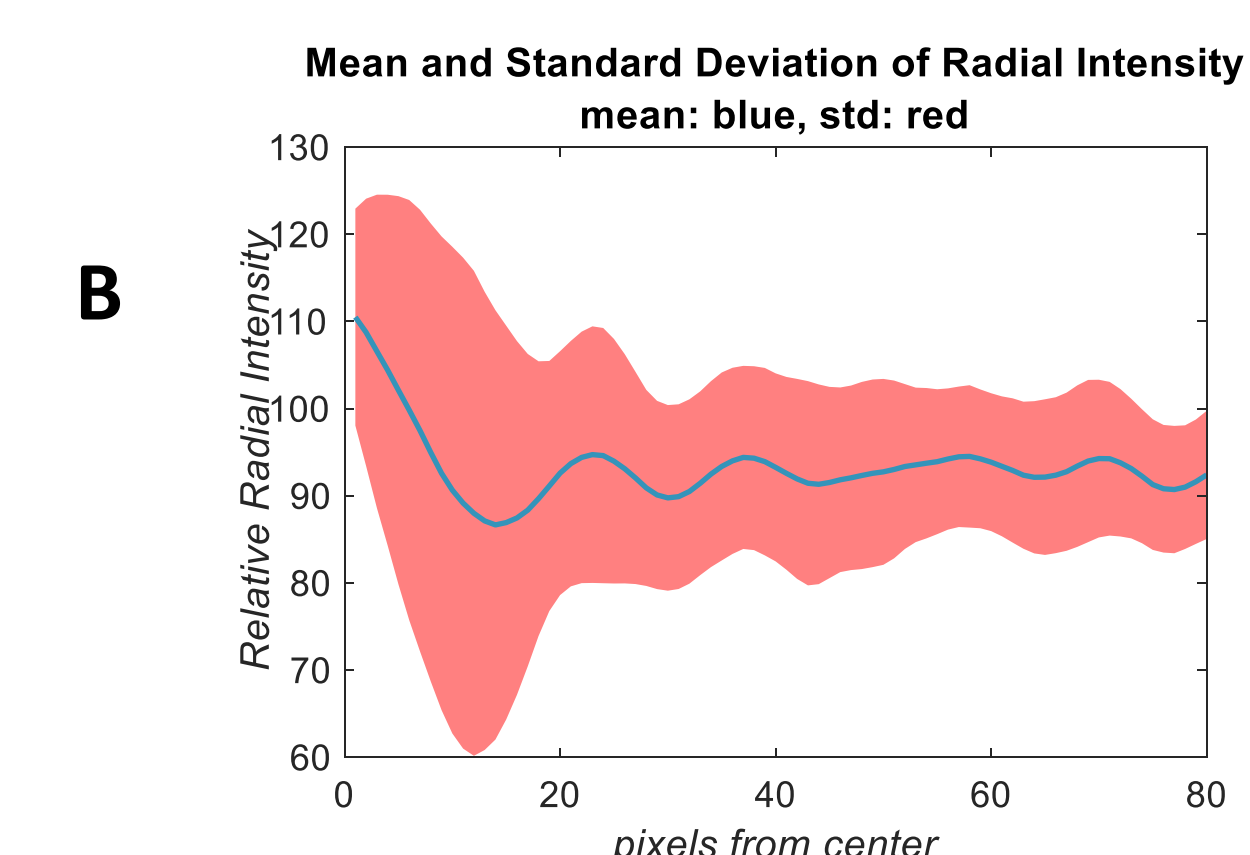
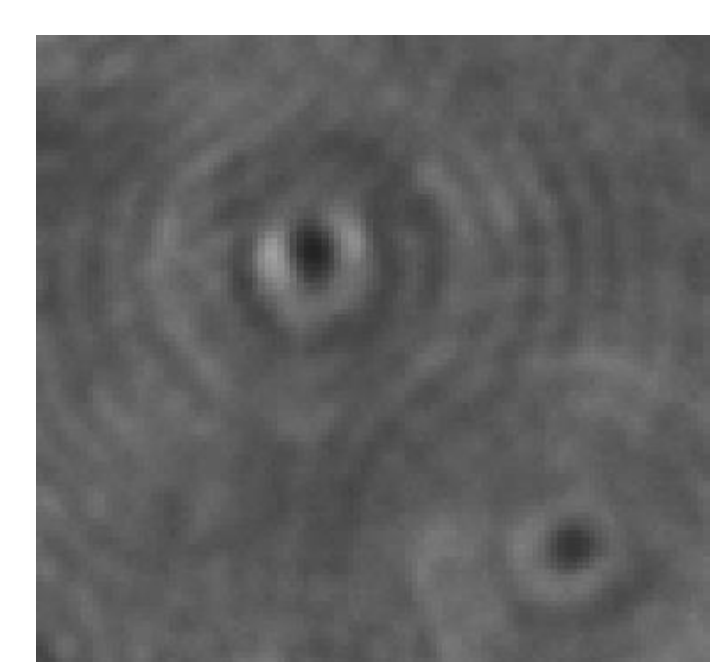
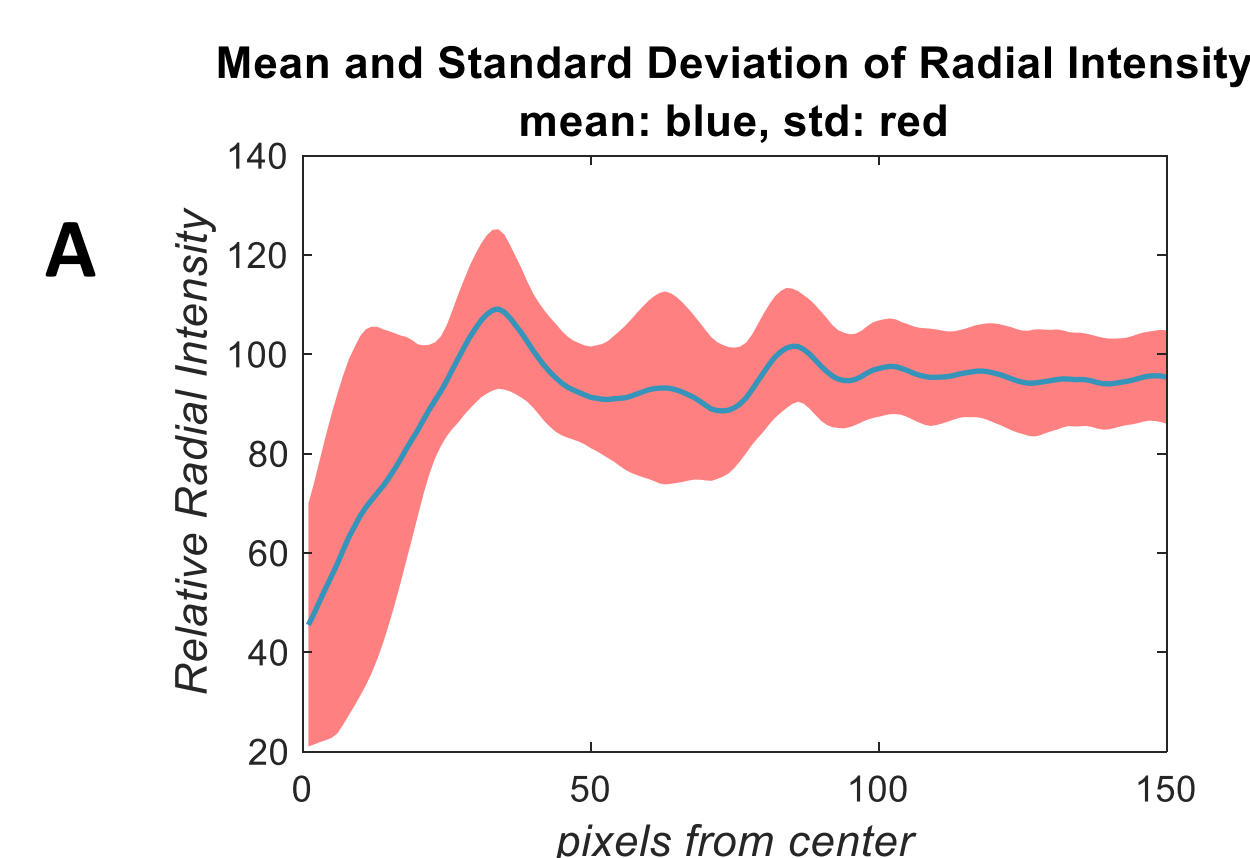
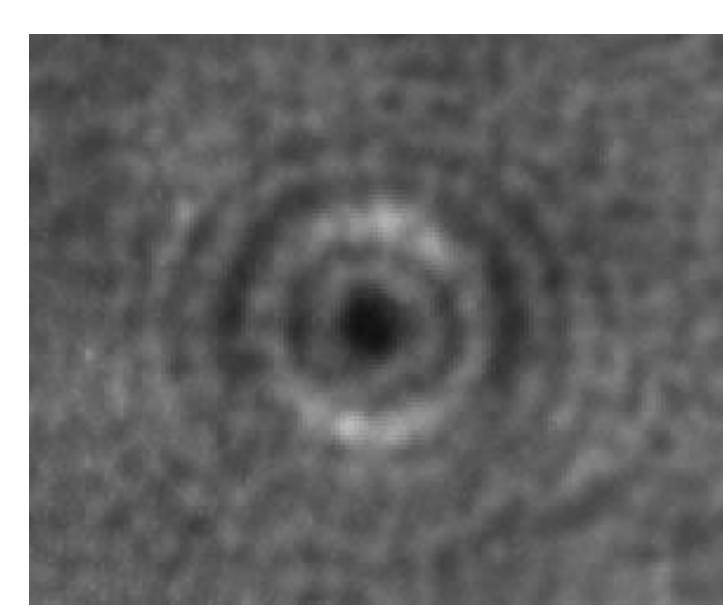


**Fig.3.A, B.:** Representation of the lens supported inline point source holographic raw image (520 nm) and the calculated polar coordinate signature of *Candida Albicans* (A) and *Escherichia Coli* (B). Blue lines indicate the mean, the red areas indicate the standard deviation of the polar coordinate values at a given pixel radius.

Pixel dimensions of the raw image:  $162.7 \pm 2.4$  nm.

### Comparison of lens-free and lens-supported simulations.

**Fig.5.** Simulated holographic particle intensity in the function of diameter

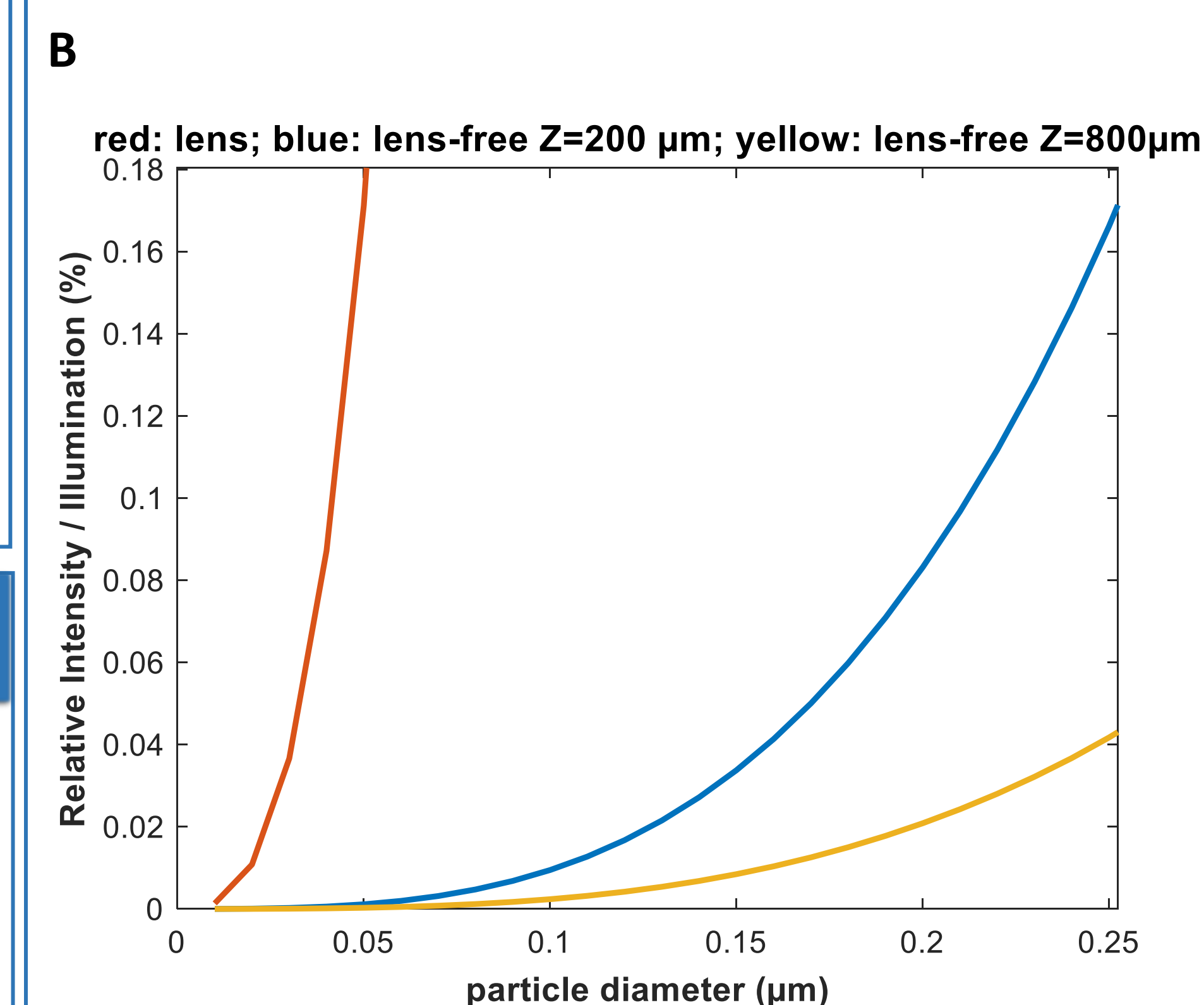
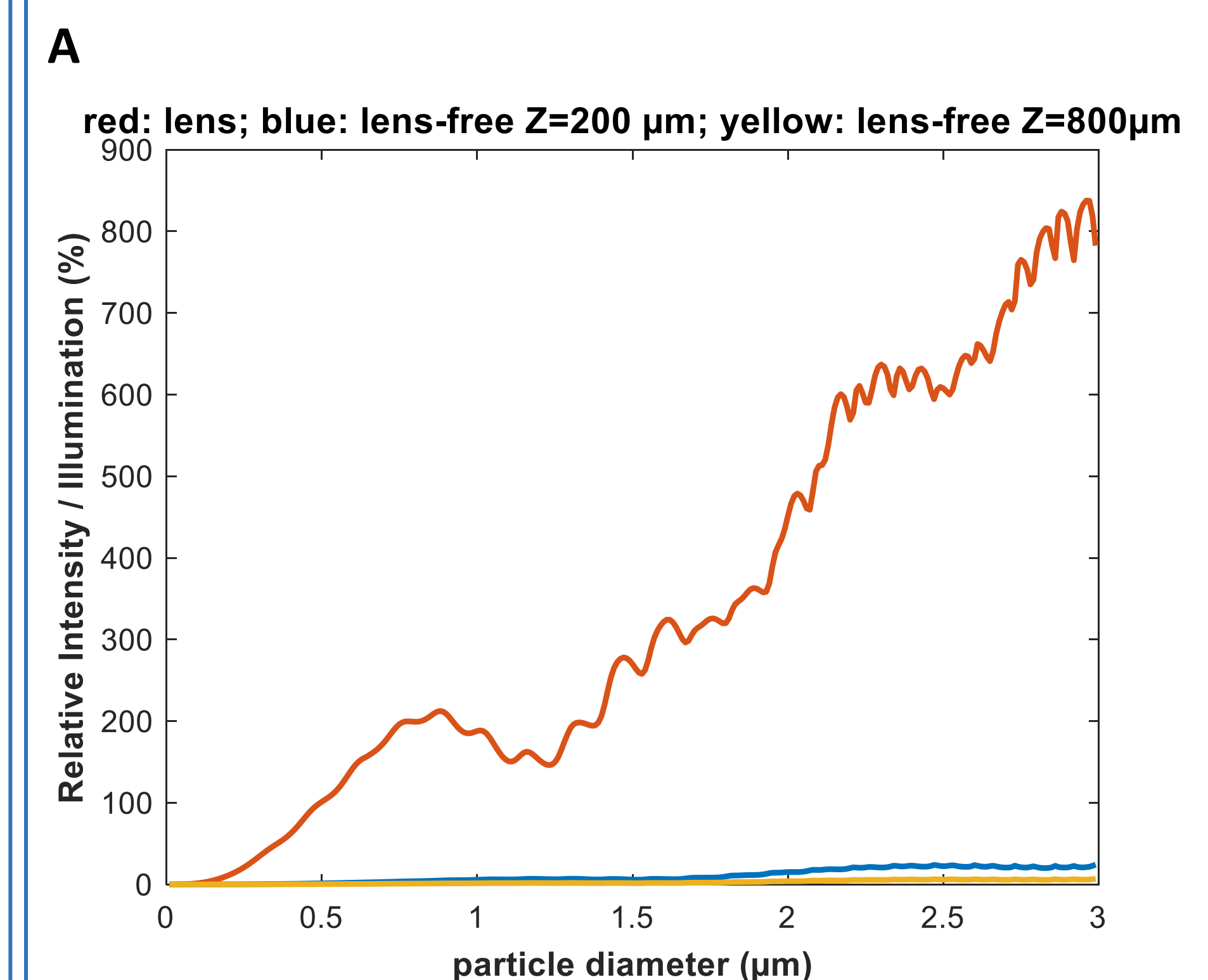


**Fig. 5. A, B.**

Relative intensity ratio of the simulated holographic raw datasets is plotted against the particle diameter. Simulations were carried out according to the 'Mie' scattering model. The wavelength of the simulated coherent laser illumination was 520 nm.

Colours indicate the measurement configuration: lens-supported (red), lens-free (blue and yellow). Distance of the particle from the detector plane (indicated by 'Z' on the figures) was 1  $\mu\text{m}$  in the case of lens-supported system and was 200  $\mu\text{m}$  and 800  $\mu\text{m}$  in the case of lens-free configuration.

### Statistical View of Detection Limit

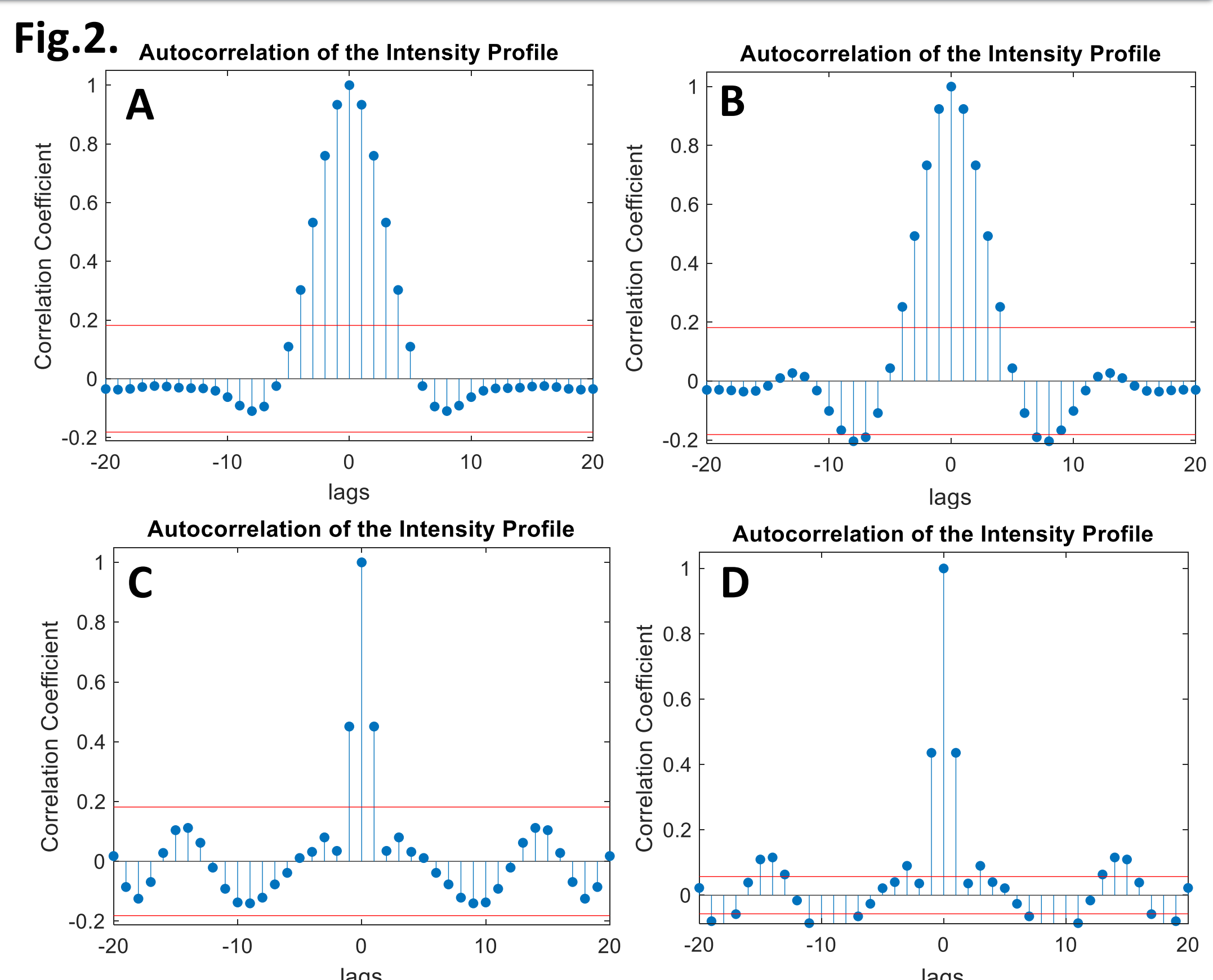


**Fig. 2. A, B, C, D.**

Autocorrelation coefficient of simulated pixel intensity profiles plotted against 'lags'. Particle diameter  $d = 2$   $\mu\text{m}$  (A);  $d = 1.5$   $\mu\text{m}$  (B);  $d = 0.125$   $\mu\text{m}$  (C);  $d = 0.05$   $\mu\text{m}$  (D).

95% confidence interval (red line) indicates that the intensity profiles are hardly different from a random process under 0.125  $\mu\text{m}$  diameter of particles. The intensity profiles are distinguishable under 95% coverage probability within the range of 1 – 2  $\mu\text{m}$  of particle diameter.

### Multidimensional comparison

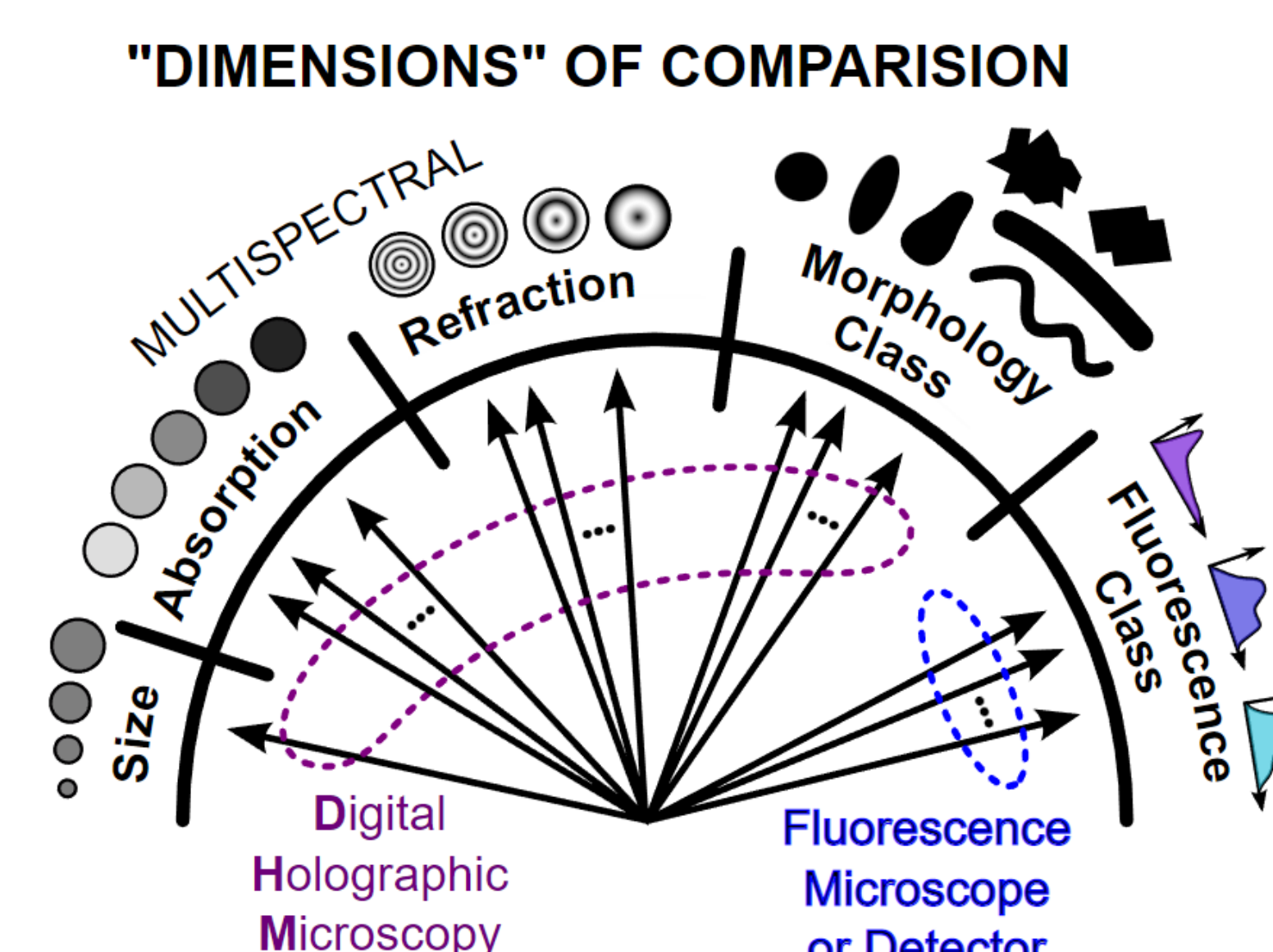


**Fig.4.** Representation of the HoloZcan workflow to define the features of objects of interest.

This Poster in PDF  $\Rightarrow$



**CORRESPONDING AUTHOR:**

Dr. János PÁLHALMI, e-mail: [janos.palhalmi@datasenselabs.net](mailto:janos.palhalmi@datasenselabs.net)

**Project HoloZcan:**

[WWW.HOLOZCAN.COM](http://WWW.HOLOZCAN.COM), e-mail: [info@HoloZcan.com](mailto:info@HoloZcan.com)